



Atmospheric nitrogen deposition in the Yangtze River basin: Spatial pattern and source attribution[☆]



Wen Xu ^{a, b, 1}, Yuanhong Zhao ^{c, 1}, Xuejun Liu ^{a, *}, Anthony J. Dore ^d, Lin Zhang ^c, Lei Liu ^e, Miaomiao Cheng ^f

^a College of Resources and Environmental Sciences, Beijing Key Laboratory of Cropland Pollution Control and Remediation, China Agricultural University, Beijing 100193, China

^b State Key Laboratory of Urban and Regional Ecology, Research Center for Eco-Environmental Sciences, Chinese Academy of Sciences, Beijing 100085, China

^c Laboratory for Climate and Ocean-Atmosphere Sciences, Department of Atmospheric and Oceanic Sciences, School of Physics, Peking University, Beijing 100871, China

^d Centre for Ecology and Hydrology, Edinburgh, Bush Estate, Penicuik, Midlothian EH26 0QB, UK

^e Jiangsu Provincial Key Laboratory of Geographic Information Science and Technology, International Institute for Earth System Science, Nanjing University, Nanjing 210023, China

^f State Key Laboratory of Environmental Criteria and Risk Assessment, Chinese Research Academy of Environmental Sciences, Beijing 100012, China

ARTICLE INFO

Article history:

Received 3 May 2017

Received in revised form

25 September 2017

Accepted 26 September 2017

Available online 6 October 2017

Keywords:

Nitrogen deposition

Source apportionment

Ecological risks

Mitigation strategy

The Yangtze River basin

ABSTRACT

The Yangtze River basin is one of the world's hotspots for nitrogen (N) deposition and likely plays an important role in China's riverine N output. Here we constructed a basin-scale total dissolved inorganic N (DIN) deposition (bulk plus dry) pattern based on published data at 100 observational sites between 2000 and 2014, and assessed the relative contributions of different reactive N (N_r) emission sectors to total DIN deposition using the GEOS-Chem model. Our results show a significant spatial variation in total DIN deposition across the Yangtze River basin ($33.2 \text{ kg N ha}^{-1} \text{ yr}^{-1}$ on average), with the highest fluxes occurring mainly in the central basin (e.g., Sichuan, Hubei and Hunan provinces, and Chongqing municipality). This indicates that controlling N deposition should build on mitigation strategies according to local conditions, namely, implementation of stricter control of N_r emissions in N deposition hotspots but moderate control in the areas with low N deposition levels. Total DIN deposition in approximately 82% of the basin area exceeded the critical load of N deposition for semi-natural ecosystems along the basin. On the basin scale, the dominant source of DIN deposition is fertilizer use (40%) relative to livestock (11%), industry (13%), power plant (9%), transportation (9%), and others (18%, which is the sum of contributions from human waste, residential activities, soil, lighting and biomass burning), suggesting that reducing NH_3 emissions from improper fertilizer (including chemical and organic fertilizer) application should be a priority in curbing N deposition. This, together with distinct spatial variations in emission sector contributions to total DIN deposition also suggest that, in addition to fertilizer, major emission sectors in different regions of the basin should be considered when developing synergistic control measures.

© 2017 Published by Elsevier Ltd.

1. Introduction

In the past few decades, human activities associated with agricultural and industrial production emitted large amounts of nitrogen (N) oxides ($\text{NO}_x = \text{NO} + \text{NO}_2$) and ammonia (NH_3) to the

atmosphere (Galloway et al., 2008). They can be transported in downwind direction and transformed in the atmosphere to nitric acid (HNO_3) and to particulate ammonium (NH_4^+) and nitrate (NO_3^-) via chemical reactions, and eventually return to earth surface by wet and dry deposition processes. As a consequence, atmospheric N deposition has dramatically increased globally, and this increase is expected to continue over China (Kanakidou et al., 2016). Meanwhile, a considerable portion of deposited N in land can also be transported to coastal waters and the open ocean via river flow (Fowler et al., 2013). Excessive N inputs into aquatic ecosystems can cause negative environmental and ecological effects, e.g.,

[☆] This paper has been recommended for acceptance by Dr. Hageman Kimberly Jill.

* Corresponding author.

E-mail address: liu310@cau.edu.cn (X. Liu).

¹ Contributed equally to this work.

eutrophication of water body (Bergström and Jansson, 2006), hypoxia (Diaz and Rosenberg, 2008), breakout of red tide (Dai et al., 2010), and a loss of biodiversity (Clark and Tilman, 2008).

The Yangtze River basin is a region characterized by rapid economic development and population growth, and generates as much as half of China's gross domestic product (GDP) (Lin et al., 2005). This, in turn, makes the basin suffered from serious reactive nitrogen (N_r) pollution (Gu et al., 2012). The Yangtze River is the largest river in the Euro-Asian continent and is the third longest river in the world. It is responsible for significant N discharges into its estuary and the adjacent East China Sea, leading to negative ecological effects (Dai et al., 2010). Dissolved inorganic nitrogen (DIN), which includes oxidized (e.g., NO_x , HNO_3 , NO_3^-) and reduced (e.g., NH_3 , NH_4^+) forms, is often the most abundant and bioavailable form of N and thereby contributes significantly to coastal eutrophication (Veuger et al., 2004; Dumont et al., 2005). Using a mass balance model, Wang et al. (2014) estimated that the contributions of bulk DIN deposition (i.e. wet plus some dry deposition, measured by open rain collectors) to total N input to the basin increased from 3% in 1980 to 5% in 2000. Furthermore, Chen et al. (2016) reported that atmospheric DIN deposition accounts for on average approximately 13% of human-controlled N inputs into the basin during the period of 1980–2012. Using principal components analysis, Xu et al. (2013) estimated that DIN deposition contributed 25–28% of total DIN loads in the river between 1972 and 2010. These estimated contributions, however, are inherently uncertain mainly due to the scarcity of complete observational data on dry N deposition, which accounted for approximately 40% of total N deposition in the Yangtze River basin (Shen et al., 2013; Xu et al., 2015; Kuang et al., 2016), compared with 60% of that in northern China (Pan et al., 2012). Indeed, long-term measurement of dry N deposition at a regional scale remains a major challenge because of the wide range of N-containing compounds in gaseous and aerosol phases, and technical difficulties associated with measurement of their deposition, especially in remote areas (Xu et al., 2015). An alternative and widely accepted approach uses a spatial interpolation technique to yield continuous estimates of dry N deposition from discrete data points on a spatial scale (Nowlan et al., 2014; Jia et al., 2016). However, to date, no study (based on the interpolation method) has provided any information on the magnitude and spatial pattern of total (wet plus dry) DIN deposition over the Yangtze River basin, significantly limiting our knowledge of the N cycle in the basin.

Chemical transport models (CTMs) are capable of simulating the magnitude and spatial pattern of total DIN deposition, and have been employed at the national scale (Zhang et al., 2012a) and on a global scale (Vet et al., 2014; Kanakidou et al., 2016). Recent advances in N deposition modeling include improved estimates of DIN deposition at a continental scale using a nested modeling approach with the GEOS-Chem global chemical transport model to estimate DIN deposition in China (Zhao et al., 2017). However, few studies modeled the spatial distribution patterns of total DIN deposition at a regional scale (Huang et al., 2015), mainly due to lack of resolution in model input data, such as spatial emissions. In addition, modeled total DIN deposition should be compared to surface observations to validate and improve models, but few of these datasets are available (Pan et al., 2012; Xu et al., 2015). Thus, application of the interpolation method and comparison with a modeling method can provide reliable information on the magnitude and spatial pattern of total DIN deposition at a regional scale.

To develop emission control strategies to conserve ecosystem health, the emission sources of N deposition needed to be determined. Using the moss $\delta^{15}N$ method, a previous study determined that the main atmospheric N sources in the Yangtze River basin were excretory wastes for most of the cities and soil emission for

forests (Xiao et al., 2010). However, large uncertainties may exist in the results from Xiao et al. (2010), since relevant analysis was built on the $\delta^{15}N$ signatures of potential atmospheric N sources established for other countries (e.g. Germany); it is unsure whether there is spatial variability of $\delta^{15}N$ signatures. Fortunately, CTMs by simulating physical and chemical processes of atmospheric N pollution are useful in providing insights into the relative contribution of emissions sources to N deposition. Existing CTMs such as the Goddard Earth Observing System with chemistry (GEOS-Chem) model (Lee et al., 2016; Zhao et al., 2017), the Community Multi-scale Air Quality (CMAQ) model (Qiao et al., 2015) and the European EMEP model (Simpson et al., 2014) have capability to link N sources with deposition. For example, Zhao et al. (2017) used the GEOS-Chem model to show that in China total N deposition is predominantly contributed by domestic anthropogenic sources (86%), followed by *trans*-boundary import of anthropogenic sources (7%) and natural sources (7%). However, relative contributions from different emission sectors (e.g., fertilizer, manure, industry, power plants, and other) to N deposition were not quantified. Source attribution data calculated with CTMs may be used in an integrated assessment modeling framework to calculate the cost-benefit of reduced nitrogen deposition from targeted emission reduction policies (Oxley et al., 2013).

In the present study, we use the spatial interpolation technique and available published data to map the spatial distribution of total DIN deposition in the Yangtze River basin. In addition to this, an attempt is made to quantify contributions from different emission sectors (i.e. fertilizer use, livestock, industry, power plant, transportation, and others) to total DIN deposition using the GEOS-Chem model. A comparison of spatial patterns of total DIN deposition obtained with interpolation technique and the GEOS-Chem model is also made using provincial deposition totals. The outcomes of this study are expected to provide the scientific basis for developing an effective policy for N pollution abatement in the basin.

2. Methodology and data collection

2.1. Study area

The Yangtze River basin is located between 24° – $35^{\circ}N$ and 90° – $122^{\circ}E$, originating from the Tibetan Plateau, cross the country from west to east, and finally flowing into the East China Sea (Fig. 1). The basin has a total drainage area of approximately 1.8×10^6 km², covering about 20% of the total land area of mainland China. The areas of the Hubei, Hunan, Jiangxi, and Sichuan provinces, which are totally located within the basin, account for about 65% of the total basin area, while areas of the other 13 provinces (Qinghai, Gansu, Yunnan, Tibet, Shaanxi, Guizhou, Guangxi, Henan, Anhui, Jiangsu, Shanghai, Guangdong, Fujian) account for 35% of the total basin area (Yan et al., 2003). The climate in large parts of the basin is subtropical monsoon. The long-term mean annual precipitation in this region is approximately 1070 mm, but the spatial and temporal distributions are highly uneven, ranging from 500 mm in the west to 2500 mm in the east, and more than 60% of the annual precipitation occurs in summer (June, July and August) (Xu et al., 2008).

There are nearly 440 million inhabitants in the basin. The main land use types are forest, farmland and grassland (Fig. 1), of which the areas accounted for 40%, 30% and 24% respectively, of the total basin area over the 1980–2012 period (Chen et al., 2016). Agriculture is well developed in the Sichuan basin and corresponding regions in the middle and lower reaches of the Hunan, Hubei, Anhui and Jiangsu provinces, where regional NH_3 emissions are concentrated compared with low NH_3 emissions in the northwest remote area of the basin (e.g., Qinghai and Xizang) (Huang et al., 2012). In these regions, a turning cultivation system of rice-wheat, rice-rape,

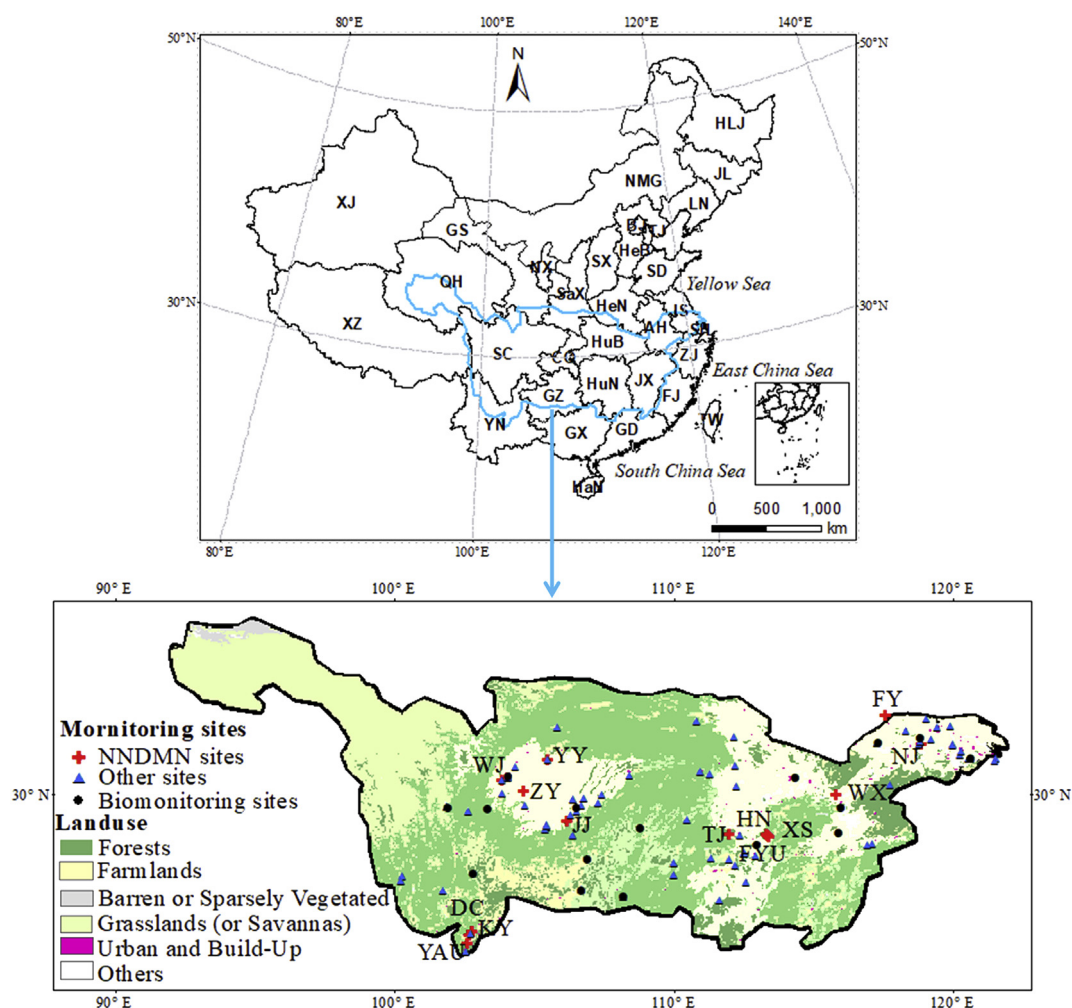


Fig. 1. Geographic location of the Yangtze River basin and the 100 monitoring sites.

rice-cotton and rice-sweet potato, along with a rotation of rice-peanut, rice-green manure, or double cropping of rice are practiced at a high cropping intensity between 200% and 250% (Liu et al., 2008). High emission density of NO_x occurs in Shanghai and Jiangsu (Zhao et al., 2013).

2.2. Data collection and description

We collected data on from published literature on DIN deposition in the Yangtze River basin during the 2000–2014 period (see Table S1 in Supplementary Information (SI) for a complete reference list). This dataset was built by surveying the peer-reviewed literature with the Web of Science (Thompson-ISI, Philadelphia, PA, USA) and CNKI website (<http://www.cnki.net/>). Briefly, keyword searches used “nitrogen deposition”, “chemical composition” or “precipitation”, and “China”. After rigorous data screening and quality control for the Yangtze River basin, a total of 100 sites were included. These sites cover urban, rural and forested areas. The geographical distribution of all selected sites is shown in Fig. 1. Our compiled dataset of DIN deposition can be divided into three categories according to the types of deposition and sampling method: dry and bulk deposition data sets, wet and bulk deposition data set, and total deposition (dry plus wet) data set. A brief description of those three sub-data sets is given below. The details of all the sites, including site name, site coordinate, monitoring

period, and land use type are presented in Table S1 in SI.

The dry and bulk deposition data sets were collected from 14 monitoring sites (Fig. 1, and numbers highlighted in red in Table S1, SI) in a Nationwide Nitrogen Deposition Monitoring Network (NNDMN) in China (Xu et al., 2015), which investigated both dry and bulk N deposition simultaneously since 2010. This network focused on five major DIN species (i.e., gaseous NH_3 , HNO_3 , NO_2 , and particulate NH_4^+ and NO_3^-) sampled using active and passive samplers, and on NH_4^+ and NO_3^- in precipitation collected using precipitation gauges. Dry deposition fluxes were estimated by combining measured N_r concentrations with simulated deposition velocity; Bulk deposition fluxes were calculated by multiplying the precipitation amount with the volume-weighted mean concentrations of NH_4^+ and NO_3^- in the precipitation.

The wet and/or bulk deposition data set was collected from 70 monitoring sites (Fig. 1, and numbers highlighted in blue in Tables S1 and SI), with the former mainly based on automatic precipitation sampling collectors and the latter mainly based on continuously-open collectors (e.g., rain gauge, bucket). In reality, the collected data at those sites were DIN concentrations in precipitation and precipitation amount. Further, we approximate wet and/or bulk deposition fluxes according to the aforementioned method. It should be noted that data on bulk deposition flux accounted for about 79% of the data set. Only 4 out of 70 sites (Sites 2, 19, 74 and 75, see Tables S1 and SI) had monitoring periods for

wet and/or bulk deposition that shorter than 1 year, but covered the local rainy season (i.e., spring and summer). Therefore, the calculated fluxes to some extent can represent their respective annual deposition levels.

The total deposition (dry plus wet) data set was collected from 16 biomonitoring sites (Fig. 1, and numbers highlighted in black in Table S1) in the study of Xiao et al. (2010), who used moss tissue N contents to estimate total DIN deposition flux for the year 2006 based on a significant linear regression equation between the estimated atmospheric N deposition and moss N content.

In line with our previous study (Xu et al., 2015), the term ‘total deposition’ in this study is also defined as the sum of dry and bulk deposition unless specified otherwise, although it is in principle defined as the sum of dry and wet deposition. The difference between bulk and wet deposition is likely small in the Yangtze River basin. For example, we compared the results from Kuang et al. (2016) and Song et al. (2017), and found that the difference between 5-year *in situ* measurements of bulk and wet DIN deposition was only about $2.5 \text{ kg N ha}^{-1} \text{ yr}^{-1}$ at a rural site, equaling to 12% of annual bulk deposition. In addition, Shen et al. (2013) found that wet DIN deposition on average accounted for nearly 85% of the bulk DIN deposition at three rural/forested sites. Therefore, the sum of dry and bulk deposition could be comparable to the sum of dry and wet deposition, and thus is termed ‘total deposition’. However, it should be noted that the bulk samplers will collect some dry deposited fine and coarse particles and gases. Therefore, total deposition derived from bulk sampling will be higher than that derived from wet and dry sampling and the bias was not evaluated.

2.3. Calculation and mapping of total DIN deposition

To calculate total DIN deposition at 70 sites with only wet and/or bulk DIN deposition measurements (Table S1, SI), it is essential to estimate dry deposition fluxes. Here we calculated dry DIN deposition fluxes by multiplying their measured wet and/or bulk deposition fluxes with a dry/bulk deposition ratio. In brief, the ratios were uniformly assumed to be 0.65, 0.94, and 0.60 for rural, urban and forest sites, which were respectively averaged from the ratios for corresponding land use types at all selected NNDMN sites except for 3 sites in Yunnan province (which show relatively higher dry/bulk ratios due to abnormal (extreme drought condition) precipitation amounts, see details in Table S1, SI). The variability in the ratios was mainly due to the differences in N_r emission intensity, weather conditions (e.g., wind speed, precipitation), underlying surface parameters (e.g., surface roughness length and land type) (Xu et al., 2015). This method has been used elsewhere (Chen et al., 2016), albeit with some uncertainties. To study the spatial pattern of total DIN deposition, we used annual average values of deposition fluxes when there were measurements more than one year in each data set (Table S1, SI).

A Kriging interpolation technique was employed to construct a regional-scale map of total DIN deposition in the Yangtze River basin (Fig. 2a). One site (i.e., FY) situated near the boundary of the Yangtze River basin (about 65 km distant, Fig. 1) was included in the analysis to decrease the effect of boundary issues on the spatial interpolation technique. Prior to Kriging interpolation, SPSS 11.5 software was used to test whether the original data accorded with normal distribution and thereby determine if a data conversion is required. Then, the Explore Data tool of ArcGIS 10.0 was employed to perform a data analysis including outlier identification and trend analysis; Geostatistics plus (GS+) was applied to determine the optimal variogram model and parameters. The results of the Kriging interpolation were evaluated using a cross-validation analysis, i.e., compared predicted value to the original measured value at all selected sites. For the area of the basin belonging to Qinghai

province, we assumed that total DIN deposition was in the range of $1\text{--}2 \text{ kg N ha}^{-1} \text{ yr}^{-1}$ due to lack of corresponding reported data. This range was extracted from our modeled total DIN deposition to China for the year 2010. Also, a recent modeling study reported that total inorganic N deposition in that area is $< 2 \text{ kg N ha}^{-1} \text{ yr}^{-1}$ over 2008–2012 period (Zhao et al., 2017). Thus, the flux used here can be assumed to be representative of the region.

All correlation analyses were performed using SPSS software (version 11.5; SPSS Inc., Chicago, IL, USA), with a significance level of $p < 0.05$.

2.4. Source attribution of N deposition

In this study, the GEOS-Chem (<http://geos-chem.org>) was used to assess the relative contributions of different emission sectors to the simulated total N deposition over the Yangtze River basin in 2010. The total DIN deposition made up about 96% of the simulated total N deposition (Table 1). For consistency when discussing modeled deposition fluxes along with the interpolated deposition fluxes, we refer to the modeled total N deposition as total DIN deposition, although we recognized here that the modeled total deposition included 4% dry organic nitrogen deposition. GEOS-Chem is a 3-D global atmospheric CTM driven by GEOS-5 assimilated meteorological data from the NASA Goddard Earth Observing System with a temporal resolution of 6 h (3 h for surface variables and mixing depths) and a horizontal resolution of $1/2^\circ$ latitude by $2/3^\circ$ longitude.

The model includes aerosol and gas-phase chemistry with heterogeneous aerosol chemistry parameterized using uptake coefficients (Jacob, 2000), and photolysis rates which are dependent on aerosol concentrations (Martin et al., 2003). Tropospheric gas-phase chemistry is represented by the $\text{O}_3\text{--NO}_x$ hydrocarbon system (Hudman et al., 2007). The ISORROPIA II thermodynamic equilibrium model of Fountoukis and Nenes (2007) is employed to represent the partitioning of total NH_3 and HNO_3 between the gas and aerosol phases. A standard resistance-in-series model is used to calculate dry deposition for gases (Wesely, 1989) and aerosols (Zhang et al., 2001). Wet deposition includes both convective updraft and large-scale precipitation scavenging as for aerosols (Liu et al., 2001) and gases (Mari et al., 2000). The nested version of GEOS-Chem has been applied to simulate nitrogen deposition in China and the adjacent ocean (Zhao et al., 2015, 2017). For example, Zhao et al. (2017) conducted a 5-year (2008–2012) comparison of surface observations and model simulations of wet deposition fluxes for China, and their results showed good agreement for wet deposition fluxes of NH_4^+ ($r = 0.56$, bias = -1%) and NO_3^- ($r = 0.70$, bias = -15%), as well as for NH_3 concentration ($r = 0.65$, bias = 4%).

Here we conduct the same GEOS-Chem simulation of N deposition as Zhao et al. (2017) for 2010 and examine the source attribution by model sensitivity tests. The model uses the Multi-Resolution Emission Inventory of China (MEIC, <http://meicmodel.org>) for anthropogenic emissions over China, except for NH_3 that are obtained from the Regional Emission in Asia (REAS-v2) inventory (Kurokawa et al., 2013). An updated seasonality described by Zhao et al. (2015) is applied to NH_3 emissions to improve the simulation. Details of the model emissions have been given in Zhao et al. (2017). Table 2 lists the total NH_3 and NO_x emissions from each source over China and the Yangtze River basin (Fig. 1). The NH_3 and NO_x emissions over the Yangtze River basin are 4.0 Tg N a^{-1} and 2.2 Tg N a^{-1} in 2010, which respectively, account for 31% and 23% of their total emissions over China. Agricultural sources including fertilizer use and livestock, comprise most of the NH_3 emissions (63% and 18%) while fuel combustion activities, including industry, power plant, and transportation contribute most of the NO_x emissions (40%, 25% and 24%) and small amounts of NH_3 emissions (5%).

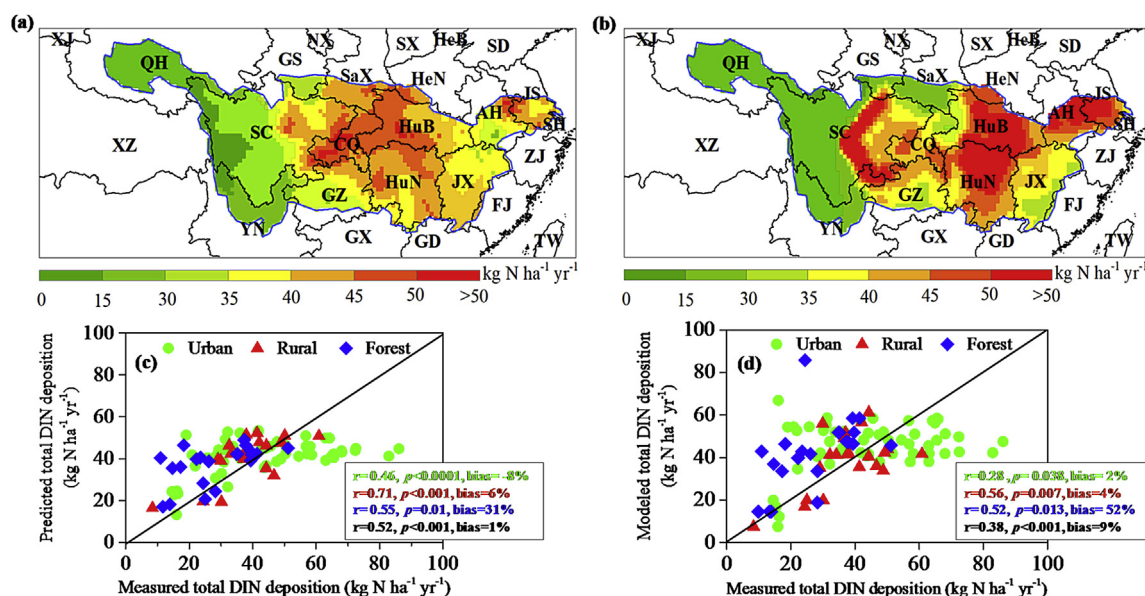


Fig. 2. Spatial patterns of total DIN deposition in the Yangtze River basin derived from the Kriging interpolation during the period of 2000–2014 (a) and the GEOS-Chem model for the year 2010 (b). The Kriging interpolated results and GEOS-Chem model results are compared with measured total DIN deposition (as given in Tables S1 and S1) as scatter-plots (c and d, bottom panels). The full names of the provinces are successively Hebei, Shandong, Gansu, Shanxi, Shanxi, Henan, Guizhou, Jiangsu, Hubei, Shanghai, Anhui, Ningxia, Jiangxi, Zhejiang, Chongqing, Sichuan, Fujian, Guangdong, Guangxi, Hunan, Yunnan, Xinjiang, Xizang, Qinghai.

Table 1
Nitrogen deposition over the Yangtze River basin.^a

	Deposition process	Deposition (kg N ha ⁻¹ yr ⁻¹)
NH _x	Total	21.9
	Wet NH ₄ ⁺	15.5
	Dry NH ₃	4.5
	Dry particulate NH ₄ ⁺	1.9
NO _y	Total	11.0
	Wet NO ₃ ⁻	7.1
	Dry HNO ₃	2.2
	Dry NO ₂	0.47
	Dry isoprene nitrates ^b	0.19
	Dry N ₂ O ₅	0.056
	Dry PANs ^c	0.11
	Dry particulate NO ₃ ⁻	0.88
	Dry alkyl nitrates	0.036

^a Annual total N deposition for 2010 computed with GEOS-Chem model.

^b Isoprene nitrates are formed via the oxidation of biogenic isoprene and are removed by wet and dry deposition at the same deposition velocity of HNO₃ in the model following Zhang et al. (2012a).

^c Peroxyacetyl nitrate (PAN) and higher peroxyacyl nitrates.

Both NH₃ and NO_x have natural sources (including lightning, biomass burning and soil emissions), but are negligible (3–4%) compared to anthropogenic emissions over the Yangtze River basin.

To assess the contributions from main N_r sources (fertilizer use, livestock, industry, power plant, and transportation), we conduct a series of model sensitivity simulations for the year 2010 with the corresponding emission sources turned off. The difference with the standard simulation (with all emissions turned on) can then represent their individual contribution to N deposition.

3. Results and discussion

3.1. Atmospheric deposition of total DIN in the Yangtze River basin

As shown in Fig. 3, across the basin total DIN deposition generated from the Kriging interpolation on average was 33.2 kg N ha⁻¹ yr⁻¹, close to the GEOS-Chem simulated deposition value

Table 2
Annual total NH₃ and NO_x emissions over China and the Yangtze River basin (Tg N a⁻¹).

	Source Type	China	Yangtze River basin
NH ₃	Fertilizer ^a	7.9	2.5
	Livestock	2.4	0.7
	Human waste	1.5	0.5
	Fuel combustion ^b	0.7	0.2
	Natural	0.5	0.1
	Total	12.9	4.0
NO _x	Industry	3.4	0.9
	Power	2.9	0.5
	Transportation	2.3	0.5
	Residential	0.4	0.1
	Natural ^c	0.8	0.1
	Total	9.6	2.2

^a Fertilizer NH₃ emissions include both chemical fertilizer and manure fertilizer.

^b NH₃ emissions from fuel combustion in power plant, industry, transportation and residential.

^c Natural NO_x emissions from soil, lightning and biomass burning.

(32.9 kg N ha⁻¹ yr⁻¹) for the year 2010. Evidence from a variety of studies confirms that the three global hotspots for atmospheric N deposition are China, West Europe and North America (Dentener et al., 2006; Vet et al., 2014; Kanakidou et al., 2016), although there is a clear downward trend in dry N deposition for Europe and North America (Jia et al., 2016). The total DIN deposition estimated in the present study (33.2 kg N ha⁻¹ yr⁻¹) is approximately 1.4–4 times greater than the estimated values for recent years in the well urbanized and industrialized eastern US (Li et al., 2016) and the N deposition hotspots of western Europe (Vet et al., 2014), and is also approximately twice China's average N deposition between 2008 and 2012 (Zhao et al., 2017) (Fig. 3). These results suggest that the basin is subjected to a high level of atmospheric N deposition and associated ecological risks.

In the basin, the spatial pattern of total DIN deposition varied significantly according to province (Fig. 2a). To evaluate this interpolated spatial pattern, we made the cross-validation analyses and

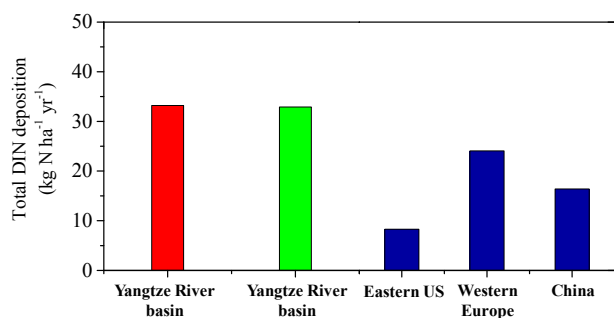


Fig. 3. Comparison of total DIN deposition observed in the Yangtze River basin and other areas (red and green bars represent interpolated and modeled values in this study; total N deposition rates in eastern US, western Europe, and China were cited from Li et al. (2106), Vet et al. (2014), and Zhao et al. (2017), respectively). (For interpretation of the references to colour in this figure legend, the reader is referred to the web version of this article.)

calculated the correlation coefficient (r) and the normalized mean bias $\text{NMB} = \frac{\text{between the measured (M) and interpolated (I) values over the 'N' (number) sites. As shown in Fig. 2c, the interpolation technique fairly reproduces the measured spatial distribution of total DIN deposition fluxes } (r = 0.52, p < 0.001), \text{ with only a small annual bias (1\%). Nevertheless, the predicted values for some sites (e.g. forest sites) were not ideal because of relatively higher root-mean-square error (14.0) (which indicates how closely the model predicts the measured values, and the smaller this error, the better. Table S2 in the Supplement) and moderate } r \text{ value.}$

For comparison with the interpolated deposition field, model simulated total DIN deposition fluxes at the model $1/2^\circ \times 2/3^\circ$ resolution for the year 2010 are mapped to the resolution of $1/2^\circ \times 1/2^\circ$ (Fig. 2b). The model also captures measured total DIN deposition fluxes ($r = 0.38, p < 0.001$) with a relatively high mean bias (10%). This is largely due to overestimates of modeled deposition fluxes at the forest sites (Fig. 2d). Interestingly, interpolated and modeled deposition fluxes were comparable in most of the areas in corresponding provinces belonging to the basin (note however that the modeled values for Guangdong and Shanghai cannot be extracted due to limitation of spatial resolution) (Fig. 4a). Furthermore, a high positive correlation ($r = 0.90, p < 0.001$) was found between interpolated and modeled deposition fluxes across corresponding provinces ($N = 17$) (Fig. 4b). This interpolation-model comparison further supports the interpolated spatial pattern of total DIN deposition and suggests that the modeled pattern can be used to fill the measurement gaps at a large spatial scale.

Based on interpolated results (Fig. 2a), most regions of the basin generally received DIN deposition $>30 \text{ kg N ha}^{-1} \text{ yr}^{-1}$. The highest fluxes of DIN deposition were concentrated in the central regions, with maximum values of $54.6 \text{ kg N ha}^{-1} \text{ yr}^{-1}$ observed in Chongqing, and the lowest deposition was observed in the under-developed regions in the west of the basin (i.e., Qinghai), with the lowest value of $1.0 \text{ kg N ha}^{-1} \text{ yr}^{-1}$. The spatial pattern observed in the present study is driven by differences in many factors, such as usage of N fertilizers, fossil fuel consumption, livestock, and precipitation as well as interregional atmospheric transport (Jia et al., 2014; Zhao et al., 2015). In addition, multiple years of measured DIN may also have a small influence on the pattern that will be discussed later (see Section 3.4). The highest annual N deposition in Chongqing is explained, in part, by the fact that Chongqing is the largest metropolitan area in southeastern China, and is featured by high emission densities of NH_3 and NO_x (Zhao et al., 2013; Kang et al., 2016). In this study, the spatial patterns of total NH_x deposition and total NO_y deposition cannot be mapped using the Kriging

interpolation due to limitation of corresponding reported data (Table S1 in the Supplement). However, the GEOS-Chem model was applied to characterize their spatial patterns. We find that there was a sharp gradient from west to east (Fig. S1 in the Supplement), consistent with reported emission patterns of NH_3 and NO_x (Zhao et al., 2013; Kang et al., 2016).

3.2. Contributions of different processes and emission sectors to total N deposition

In the present study, deposition amounts of individual N_r species (e.g., gaseous NH_3 , HNO_3 , and NO_2 , particulate NH_4^+ and NO_3^- , and rainwater $\text{NH}_4^+\text{-N}$ and $\text{NO}_3^-\text{-N}$) cannot be separated from interpolated total DIN deposition fluxes. Instead, we examine the different processes and sources contributing to total DIN deposition over the Yangtze River basin by using the GEOS-Chem model results for the year 2010. We evaluate the model simulations by comparing with observed wet (both NH_4^+ and NO_3^-) and total DIN deposition fluxes listed in Table S1 in the Supplement. The model biases were 22% for wet NH_4^+ deposition, 23% for wet NO_3^- deposition and 9% for total DIN deposition (Fig. S2 in the Supplement). These biases are reasonable and can be partially explained by the differences in N_r emissions and meteorology. Given that model evaluation is not central to this work, we presented the details in Text S1 in the Supplement.

Table 1 presents the annual total deposition amounts from individual species and from each process over the basin. On a basin scale, NH_x removal was dominated by wet deposition compared with dry deposition (15.5 versus $6.6 \text{ kg N ha}^{-1} \text{ yr}^{-1}$, respectively). Gaseous NH_3 accounted for 70% of NH_x dry deposition ($4.5 \text{ kg N ha}^{-1} \text{ yr}^{-1}$). Similar to NH_x , more NO_y was removed by wet deposition than dry deposition (7.1 versus $4 \text{ kg N ha}^{-1} \text{ yr}^{-1}$, respectively). Annually HNO_3 (56%) was the biggest contributor to NO_y dry deposition, followed by particulate NO_3^- (22%), NO_2 (12%) and others (10%). Our results show that wet deposition accounted for 71% of NH_x deposition, 65% of NO_y deposition, and 69% of the total N deposition to the basin, which is consistent with the findings of previous measurements in the basin (Xu et al., 2015). This, in turn, indicates that the bias of N deposition in the basin is likely small in the interpolated spatial pattern of the total DIN deposition, despite uncertainties in bulk measurements (e.g., amount of dry deposition fraction).

Fig. 5 shows the spatial footprint of different N_r emission sectors contributing to total DIN deposition conducted from the GEOS-Chem simulation. Emissions from fertilizer use (40%), followed by industry (13%) and livestock (11%), contribute most to N deposition over the Yangtze River basin. Power plant and transportation contribute 9% each, and other sources, including human waste, residential activities and natural sources (soil, lighting and biomass burning), contribute the remaining 18%. In addition, there were significant spatial variations in contributions of N_r emission sectors to total DIN deposition. To the east of the Qionglai mountains (northwestern rim of the Sichuan basin), the relative contributions from fertilizer use are highest (30–50%). Livestock, industry, power plant and transportation show comparable contribution of 10–20%. To west of the Qionglai mountains, where N deposition rate is relatively low, most of nitrogen deposition is from livestock (20–30%) and others sources such as human waste and residential activities (20–50%). Contributions from fertilizer use and transportation are generally less than 10% and from industry and power plant are negligible.

Since atmospheric lifetimes of particulate NH_4^+ and NO_3^- are longer than those of gaseous NH_3 and NO_x (Fowler et al., 2013), the gas-to-particle NH_3 partitioning could have a non-linear influence on N deposition. For example, if all NO_x sources were turned off

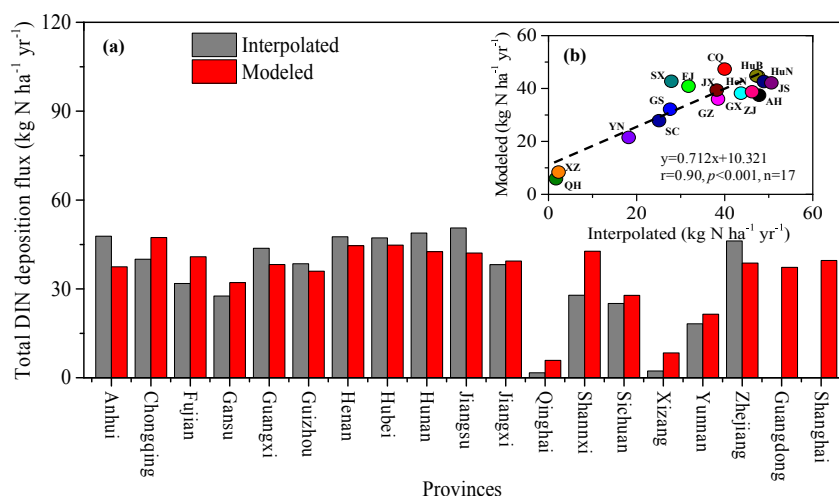


Fig. 4. A comparison of total DIN deposition from the Kriging interpolation and the GEOS-Chem model for the areas in corresponding provinces belonging to the Yangtze River basin (a) and the correlation between them (b).

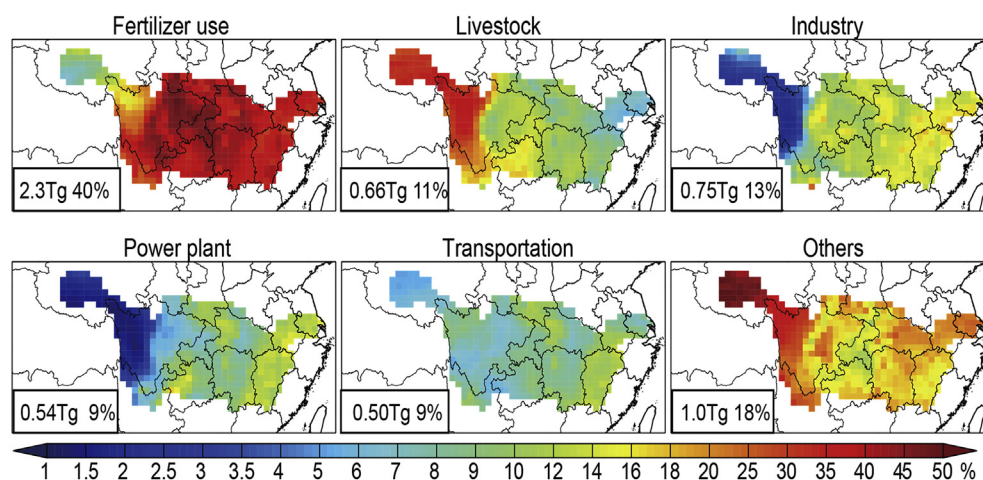


Fig. 5. Fractional contributions to total N deposition from emission sectors (i.e. fertilizer use, livestock, industry, power plant, transportation, and others including emissions from human waste, residential activities, soil, lighting and biomass burning) in the Yangtze River basin.

then there would be less NH_4^+ formation resulting in higher NH_3 deposition closer to sources. To test the influences of the nonlinearity between the emissions and deposition on source attribution results, we conducted two separate simulations which reduce the emissions from fertilizer use and industry by 20%, respectively. The simulation results show 0.46 Tg and 0.15 Tg reduction of N deposition compared with simulations with all emissions turned on, equal to 20% of total contribution from fertilizer use (2.3 Tg) and industry (0.75 Tg). These results indicate that the nonlinearity between emissions and deposition at such regional scale can be neglected for short-lived N_r species. But if we consider smaller region or deposition of individual species, the nonlinearity cannot be neglected. A detailed linearity test for the relation between emissions and deposition are recommended in future work.

Many studies have found that anthropogenic activities are main contributors to atmospheric N deposition based on CTMs simulations (Zhang et al., 2012a; Lee et al., 2016; Zhao et al., 2017), isotope techniques (Xiao et al., 2010), and/or the Positive Matrix Factorization (PMF) model (Liu et al., 2016a). For instance, using the PMF method, Liu et al. (2016a) determined the main sources of bulk DIN deposition across China during the period 2003–2014; they

reported that agricultural activities were the main contributor for NH_4^+ -N (85.9%), and NO_3^- -N was mainly from fossil fuel combustion (86.0%). In the present study, the source attribution results indicate that agricultural activities, either fertilizer use or livestock management, dominate total DIN deposition in the Yangtze River basin. The results also highlight that the intensive agriculture activities may lead to adverse environmental effects such as perturbation to the N cycle in the basin and further threaten the ecology health of the aquatic ecosystems. Recent field measurement also found that more reduced N was deposited than oxidized N in northern China (Pan et al., 2012) and even across China (Xu et al., 2015), although the ratio of NH_4^+ -N/ NO_3^- -N in precipitation decreased since the 1980s (Liu et al., 2013; Liu et al., 2016a).

3.3. Potential ecological risks of atmospheric N deposition

Critical load is a quantitative estimate of exposure to N deposition below which significant harmful ecological effects on an ecosystem do not occur over the long term (Liu et al., 2011) and have been widely used as a useful tool in evaluating the impact of N deposition on ecosystems (Duan et al., 2002; Ellis et al., 2013). In

this study, the basin was divided into five sensitive regions by the critical load of N deposition for terrestrial ecosystems in China (Table 3). Regions corresponding to 70.3% of the basin were in insensitive areas (i.e., high insensitivity and insensitivity) zones, whereas 12.0% of the basin was in slight sensitive zones. These results indicate that total DIN deposition in approximately 82% of the basin exceeded the critical loads of N deposition in terrestrial ecosystems, which mostly ranged from 10 to 20 kg N ha⁻¹ yr⁻¹ (Bobbink et al., 2010). By contrast, according to the results from current modeling studies, N deposition rate in 11% of the world's land surface exceed the critical load of 10 kg N ha⁻¹ a⁻¹ (Dentener et al., 2006), and the area which received this load accounted for between 35% and 47% of the total area of the US (Zhang et al., 2012a) and China (Zhao et al., 2017), respectively. These results indicate that a more serious potential risk of N saturation may exist in the Yangtze River basin compared with other regions in China and the world. A condition of N saturation has been detected in high N deposition areas of the basin, such as Chongqing and the Tuojiang/Minjiang River (Duan et al., 2016).

If the growth rate of N deposition in the entire basin (excluding corresponding areas in Qinghai province) coincides with the annual average growth rate of 0.36 kg N ha⁻¹ yr⁻¹ (unpublished data) derived from 5-year (2011–2015) *in situ* measurements of total DIN deposition at 9 NNDMN monitoring sites (which include NJ, WJ, WX, TJ, ZY, YT, JJ, HN and XS sites, Fig. 1) in the basin, all regions will receive N deposition exceeding 10 kg N ha⁻¹ yr⁻¹ after 25 years. The critical loads of N in the basin can be derived from estimated N critical loads for N deposition in various ecosystems in China (Liu et al., 2011; Zhao et al., 2017). Based on field observations, for example, an empirical N critical load map of N deposition drawn by Liu et al. (2011) shows that estimated values in the basin were generally >200 kg N ha⁻¹ yr⁻¹ for croplands, and <100 and 50 kg N ha⁻¹ yr⁻¹ for forests and grasslands, respectively. According to Zhao et al. (2017), the N critical load for soil eutrophication estimated using the steady-state mass balance method varied from 8 kg N ha⁻¹ yr⁻¹ to 100 kg N ha⁻¹ yr⁻¹ in the basin. Nevertheless, the critical loads for N in ecosystems are still subject to large uncertainties in the calculation methods (e.g., the SSMB), such as plant uptake rate, weathering rate, and denitrification rate (Zhao et al., 2017).

3.4. Uncertainty and recommendations

The present study reported the spatial pattern of total DIN deposition in the Yangtze River basin, the estimated flux here, however, is subject to some uncertainties in our estimation of dry deposition at the selected 70 sites, which were calculated based on dry/wet deposition ratios at their surrounding NNDMN sites. This is because the relative contribution of dry vs. wet deposition to the total deposition at a point scale largely depends on the local environment, such as N_r emissions, weather conditions (e.g.,

precipitation, wind speed) and underlying surface (Pan et al., 2012). It should be noted that the calculated wet deposition at those sites in fact are mostly bulk deposition. The wet deposition refers strictly to wet-only deposition which is sampled only during rainfall and snowfall events. Bulk deposition should be higher than actual wet deposition (Liu et al., 2015). For example, the annual difference between bulk and wet deposition was 1.3–9.6 kg N ha⁻¹ in agro-ecosystems in northern China, accounting for 5–32% of bulk deposition (Liu et al., 2017). As mentioned in Section 2.2, the difference between bulk and wet N deposition is likely small in the basin, but the use of bulk deposition may also result in uncertainties in our estimation of total DIN deposition.

Furthermore, our study pulled together DIN deposition results from a number of different field studies (Table S1 in the Supplement), which could introduce potential biases in the spatial pattern of total DIN deposition, owing to differences in monitoring, sampling handling and analysis methods. To test whether the use of data measured during 2000–2014 period could bias the spatial patterns of total DIN deposition, we summarize data on bulk DIN deposition during the period 2000–2014 from recent publications (Liu et al., 2013; Xu et al., 2015; Song et al., 2017). A total of 126 records on annual bulk DIN deposition fluxes at 43 monitoring sites were obtained (Fig. S3a in the Supplement). A non-significant trend ($p = 0.315$) can be seen for annual bulk deposition fluxes at a regional scale (Fig. S3b in the Supplement). Further, annual trends of bulk DIN deposition at five *in situ* monitoring sites (i.e., WJ, GG, JYS, GYQ, NJ) were not significant, and the similar phenomenon was also observed at two *in situ* monitoring sites for wet deposition (Fig. S3a in the Supplement). Based on these findings, we conclude that using DIN deposition measured in different years may have a little influence on the spatial pattern of total DIN deposition. On the other hand, the large-size particulate (e.g. dust or aerosols larger than 5 μm) N was normally not collected in the dry deposition collection. From this viewpoint, the overestimated “wet” deposition could be partly compensated by the underestimated “dry” deposition. To obtain more accurate information on the spatial pattern, it is crucial to establish a long-term regional N deposition monitoring network covering both wet-only and complete dry deposition using uniform monitoring methods, and to estimate deposition fluxes use a joint method of monitoring, modeling and/or spatial interpolation. In addition, it is indispensable to set up more representative observation sites in corresponding regions in the western Sichuan basin and Qinghai province where observation sites are currently absent.

Organic nitrogen (ON), which is an important component of the atmospheric N cycle (Neff et al., 2002), is not considered in the present study. Water-soluble ON contributes on average about 25% of the total dissolved N in wet deposition globally (Jickells et al., 2013), and approximately 25% of bulk N deposition in China (Zhang et al., 2012b). This soluble ON contains a wide range of N_r compounds (e.g., amino acids, amines, nitrophenols, alkyl amides, and organic nitrates) with different properties and origin (Cape et al., 2011; Jickells et al., 2013). According to the results from the first global model of atmospheric ON (Kanakidou et al., 2012), the major contributors of atmospheric ON were combustion sources (40%), primary biogenic particles (32%), and ocean particulate emissions (20%). However, a national emission inventory of ON species has not yet been developed for China. Further research is required to fill knowledge gaps of organic N emissions, which will be beneficial for source analysis of atmospheric ON deposition, an issue which remains uncertain in China.

Uncertainties also exist in the source attribution calculated with the GEOS-Chem simulations, since results largely depend on the emission inventories fed to the model. Zhao et al. (2017) pointed out that uncertainties in current NH₃ emissions inventories (e.g.

Table 3
Sensitivity of atmospheric N deposition in the Yangtze River basin and the percentage of the critical load area to the total river basin area.

Sensitivity classification	Critical loads (kg N ha ⁻¹ yr ⁻¹) ^a	Ratio of critical load area to total river basin area
High insensitivity	>40	43.1%
Insensitivity	30–40	27.2%
Slight sensitivity	20–30	12.0%
Sensitivity	10–20	8.8%
High sensitivity	<10	8.9%

^a Critical loads of atmospheric N deposition for terrestrial ecosystem in China (Duan et al., 2002).

large range of the emission value in current studies and absence of inclusion of bi-directional NH_3 exchange in land-atmosphere) may influence the nitrogen deposition simulation in China. We also point out here the high contribution (40%) from fertilizer use includes both NH_3 emissions from chemical fertilizer and manure, as they are merged into 'fertilizer use' sector in the REAS-V2 emission inventory. Future work to improve NH_3 emission inventories is needed to better simulate the spatial distribution and source attribution of N deposition in China.

3.5. Conclusions and implications for controlling regional N deposition

In summary, we have presented the spatial pattern of total DIN deposition in the Yangtze River basin based on three date sets on DIN deposition for the period of 2000–2014 at the 100 sites, and also have examined sources of total DIN deposition in the basin for the year 2010 using the GESO-Chem model at horizontal resolution of $1/2^\circ \times 2/3^\circ$. We find that there is a significant spatial variation in total DIN deposition across the basin, with the highest fluxes mainly concentrated in the central region. At a regional scale, the total DIN deposition flux was $33.2 \text{ kg N ha}^{-1} \text{ yr}^{-1}$. Meanwhile, the deposition fluxes in nearly 82% of the basin exceeded the critical loads for generic terrestrial ecosystems. Based on these findings, we propose that mitigation strategies are urgently needed in the basin and should be developed through a regional strategy according to local economical, ecological and environmental conditions. In other words, more stringent emission controls should be implemented in N emission hotspots near sensitive areas (e.g. the central regions of the basin and the Yangtze Delta) whereas moderate controls in areas near low N deposition levels (e.g. corresponding areas in Qinghai province). In this way, it could achieve a more ideal control effect without affecting the regional economic development.

The source attribution conducted by GEOS-Chem model can provide useful information for develop effective measures to reduce the excessive N_r input to the Yangtze River basin. In a regional scale, fertilizer use contributed 40% of total DIN deposition to the basin. This result provides direct evidence that reducing fertilizer NH_3 volatilization over the regional scale, by use of urease inhibitor (Li et al., 2017) and/or approximate fertilization pattern (e.g., fertilizing with a suitable choice of chemical, at the correct application level, selecting the best of the year and location) is a promising approach to decrease NH_3 emission and subsequent N deposition. Thus, in a sense, the implemented "Zero Increase Action Plan" by the Ministry of Agriculture for national fertilizer use to some extent can suppress the regional N_r pollution and N deposition (Liu et al., 2016b). In addition, manure management in feedlots to treat and use it as fertilizer to cropland should be improved. However, the fact that significant variability in emission source contributions to N deposition were observed across the study area suggests that policy-makers should also consider emission reduction from other major emission sectors in addition to fertilizer when developing synergistic control measures.

Overall, our results show that the Yangtze River basin is a N deposition hotspot in China and globally, primarily due to high levels of NH_3 emissions from improper fertilize use. Further research at a regional scale to consider both inorganic and organic N in wet and dry deposition is required to assess the spatial pattern of N deposition and optimize control strategy for protecting aquatic and terrestrial ecosystems.

Acknowledgments

This study was supported by the National Key R&D Program of China (2017YFC0210101, 2014BC954202), the National Natural

Science Foundation of China (41705130, 41425007, 31421092) as well as the National Ten-thousand Talents Program of China (XJ Liu).

Appendix A. Supplementary data

Supplementary data related to this article can be found at <https://doi.org/10.1016/j.envpol.2017.09.086>.

References

- Bergström, A.K., Jansoon, M., 2006. Atmospheric nitrogen deposition has caused nitrogen enrichment and eutrophication of lakes in the northern hemisphere. *Glob. Change Biol.* 12, 635–643.
- Bobbink, R., Hicks, K., Galloway, J., Spranger, T., Alkemade, R., Ashmore, M., Bustamante, M., Cinderby, S., Davidson, E., Dentener, F., 2010. Global assessment of nitrogen deposition effects on terrestrial plant diversity: a synthesis. *Ecol. Appl.* 20 (1), 30–59.
- Cape, J.N., Cornell, S.E., Jickells, T.D., Nemitz, E., 2011. Organic nitrogen in the atmosphere—where does it come from? A review of sources and methods. *Atmos. Res.* 102 (1–2), 30–48.
- Chen, F., Hou, L.J., Liu, M., Zheng, Y.L., Yin, G.Y., Lin, X.B., Li, X.F., Zong, H.B., Deng, F.Y., Gao, J., 2016. Net anthropogenic nitrogen inputs (NANI) into the Yangtze River basin and the relationship with riverine nitrogen export. *J. Geophys. Res. Biogeosci.* 121. <https://doi.org/10.1002/2015JG003186>.
- Clark, C.M., Tilman, D., 2008. Loss of plant species after chronic low-level nitrogen deposition to prairie grasslands. *Nature* 451 (7179), 712–715.
- Dai, Z.J., Du, J.Z., Zhang, X.L., Su, N., Li, J.F., 2010. Variation of riverine material loads and environmental consequences on the Changjiang (Yangtze) estuary in recent decades (1955–2008). *Environ. Sci. Technol.* 45 (1), 223–227.
- Dentener, F., Drevet, J., Lamarque, J.F., Bey, I., Eickhout, B., Fiore, A.M., Hauglustaine, D., Horowitz, L.W., Krol, M., Kulshrestha, U.C., Lawrence, M., GalyLacaux, C., Rast, S., Shindell, D., Stevenson, D., Van Noije, T., Atherton, C., Bell, N., Bergman, D., Butler, T., Cofala, J., Collins, B., Daherty, R., Ellingsen, K., Galloway, J., Gauss, M., Montanaro, V., Müller, J.F., Pitari, G., Rodriguez, J., Sanderson, M., Solomon, F., Strahan, S., Schultz, M., Sudo, K., Szopa, S., Wild, O., 2006. Nitrogen and sulfur deposition on regional and global scales: a multi-model evaluation. *Glob. Biogeochem. Cycles* 20, GB4003.
- Diaz, R.J., Rosenberg, R., 2008. Spreading dead zones and consequences for marine ecosystems. *Science* 321, 926–929.
- Duan, L., Hao, J., Xie, S., Zhou, Z., 2002. Estimating critical loads of sulfur and nitrogen for Chinese soils by steady state method. *Environ. Sci.* 23 (2), 7–12 (in Chinese).
- Duan, L., Chen, X., Ma, X.X., Zhao, B., Larssen, T., Wang, S.X., Ye, Z.X., 2016. Atmospheric S and N deposition relates to increasing riverine transport of S and N in southwest China: implications for soil acidification. *Environ. Pollut.* 218, 1191–1199.
- Dumont, E., Harrison, J.A., Kroeze, C., Bakker, E.J., Seitzinger, S.P., 2005. Global distribution and sources of dissolved inorganic nitrogen export to the coastal zone: results from a spatially explicit, global model. *Glob. Biogeochem. Cycles* 19, GB4502.
- Ellis, R.A., Jacob, D.J., Sulprizio, M.P., Zhang, L., Holmes, C.D., Schichtel, B.A., Blett, T., Porter, E., Pardo, L.H., Lynch, J.A., 2013. Present and future nitrogen deposition to national parks in the United States: critical load exceedances. *Atmos. Chem. Phys.* 13 (4), 9151–9178.
- Fountoukis, C., Nenes, A., 2007. ISORROPIA II: a computationally efficient thermodynamic equilibrium model for K^+ - Ca^{2+} - Mg^{2+} - NH_4^+ - Na^+ - SO_4^{2-} - NO_3^- - Cl^- - H_2O aerosols. *Atmos. Chem. Phys.* 7 (17), 4639–4659.
- Fowler, D., Coyle, M., Skiba, U., Sutton, M.A., Cape, J.N., Reis, S., Sheppard, L.J., Jenkins, A., Grizzetti, B., Galloway, J.N., Vitousek, P., Leach, A., Bouwman, A.F., Butterbach-Bahl, K., Dentener, F., Stevenson, D., Amann, M., Voss, M., 2013. The global nitrogen cycle in the twenty-first century. *Philos. T. R. Soc. B* 368 (1621), 20130164.
- Galloway, J.N., Townsend, A.R., Erisman, J.W., Bekunda, M., Cai, Z.C., Freney, J.R., Martinelli, L.A., Seitzinger, S.P., Sutton, M.A., 2008. Transformation of the Nitrogen Cycle: recent trends, questions, and potential solutions. *Science* 320 (5878), 889–892.
- Gu, B.J., Ge, Y., Ren, Y., Xu, B., Luo, W.D., Jiang, H., Gu, B.H., Chang, J., 2012. Atmospheric reactive nitrogen in China: sources, recent trends, and damage costs. *Environ. Sci. Technol.* 46 (17), 9240–9247.
- Huang, X., Song, Y., Li, M.M., Li, J.F., Huo, Q., Cai, X.H., Zhu, T., Hu, M., Zhang, H.S., 2012. A high-resolution ammonia emission inventory in China. *Glob. Biogeochem. Cy.* 26, GB1030. <https://doi.org/10.1029/2011GB004161>.
- Huang, Z.J., Wang, S.S., Zheng, J.Y., Yuan, Z.B., Ye, S.Q., Kang, D.W., 2015. Modeling inorganic nitrogen deposition in Guangdong province, China. *Atmos. Environ.* 109, 147–160.
- Hudman, R.C., Jacob, D.J., Turquety, S., Leibensperger, E.M., Murray, L.T., Wu, S., Gilliland, A.B., Avery, M., Bertram, T.H., Brune, W., Cohen, R.C., Dibb, J.E., Flocke, F.M., Fried, A., Holloway, J., Neuman, J.A., Orville, R., Perring, A., Ren, X., Sachse, G.W., Singh, H.B., Swanson, A., Wooldridge, P.J., 2007. Surface and lightning sources of nitrogen oxides over the United States: magnitudes,

- chemical evolution, and outflow. *J. Geophys. Res.* 112, D12S05. <https://doi.org/10.1029/2006jd007912>.
- Jacob, D.J., 2000. Heterogeneous chemistry and tropospheric ozone. *Atmos. Environ.* 34, 2131–2159.
- Jia, Y.L., Yu, G.R., He, N.P., Zhan, X.Y., Fang, H.J., Sheng, W.P., Zuo, Y., Zhang, D.Y., Wang, Q.F., 2014. Spatial and decadal variations in inorganic nitrogen wet deposition in China induced by human activity. *Sci. Rep.* 4 (1), 3763.
- Jia, Y.L., Yu, G.R., Gao, Y.N., He, N.P., Wang, Q.F., Jiao, C.C., Zuo, Y., 2016. Global inorganic nitrogen dry deposition inferred from ground and space-based measurements. *Sci. Rep.* 6 (6), 19810.
- Jickells, T., Baker, A.R., Cape, J.N., Cornell, S.E., Nemitz, E., 2013. The cycling of organic nitrogen through the atmosphere. *Philos. Trans. R. Soc. B* 368, 20130115.
- Kanakidou, M., Duce, R.A., Prospero, J.M., Baker, A.R., Benitez-Nelson, B., Dentener, F.J., Hunter, K.A., Liss, P.S., Mahowald, N., Okin, G.S., Sarin, M., Tsigaridis, K., Uematsu, M., Zamora, L.M., Zhu, T., 2012. Atmospheric fluxes of organic N and P to the global ocean. *Glob. Biogeochem. Cy.* 26 <https://doi.org/10.1029/2011GB004277>. GB3026.
- Kanakidou, M., Myriokefalitakis, S., Daskalakis, N., Fanourgakis, G., 2016. Past, present, and future atmospheric nitrogen deposition. *J. Atmos. Sci.* 73 (5), 160303130433005.
- Kang, Y.N., Liu, M.X., Song, Y., Huang, X., Yao, H., Cai, X.H., Zhang, H.S., Kang, L., Liu, X.J., Yan, X.Y., He, H., Zhang, Q., Shao, M., Zhu, T., 2016. High-resolution ammonia emissions inventories in China from 1980 to 2012. *Atmos. Chem. Phys.* 16 (4), 2043–2058.
- Kuang, F., Liu, X., Zhu, B., Shen, J., Pan, Y., Su, M., Goulding, K., 2016. Wet and dry nitrogen deposition in the central Sichuan Basin of China. *Atmos. Environ.* 143, 39–50.
- Kurokawa, J., Ohara, T., Morikawa, T., Hanayama, S., Janssens-Maenhout, G., Fukui, T., Kawashima, K., Akimoto, H., 2013. Emissions of air pollutants and greenhouse gases over Asian regions during 2000–2008: regional emission inventory in Asia (REAS) version 2. *Atmos. Chem. Phys.* 13 (4), 11019–11058.
- Lee, H.M., Paulot, F., Henze, D.K., Travis, K., Jacob, D.J., Pardo, L.H., Schichtel, B.A., 2016. Sources of nitrogen deposition in Federal Class I areas in the US. *Atmos. Chem. Phys.* 15 (16), 23089–23130.
- Li, Y., Schichtel, B.A., Walker, J.T., Schwede, D.B., Chen, X., Lehmann, C.M., Puchalski, M.A., Gay, D.A., Collett, J.L., 2016. Increasing importance of deposition of reduced nitrogen in the United States. *Proc. Natl. Acad. Sci. U.S.A.* 113 (21), 5874.
- Li, Q.Q., Cui, X.Q., Liu, X.J., Roelcke, M., Pasda, G., Zerulla, W., Wissemeyer, A.H., Chen, X.P., Goulding, K., Zhang, F.S., 2017. A new urease-inhibiting formulation decreases ammonia volatilization and improves maize nitrogen utilization in North China Plain. *Sci. Rep.* 7, 43853.
- Lin, Z.H., Levy, J.K., Xu, X.K., Zhao, S.X., Hartmann, J., 2005. Weather and seasonal climate prediction for flood planning in the Yangtze River Basin. *Stoch. Environ. Res. Risk Assess.* 19, 428–437.
- Liu, H.Y., Jacob, D.J., Bey, I., Yantosca, R.M., 2001. Constraints from Pb-210 and Be-7 on wet deposition and transport in a global three-dimensional chemical tracer model driven by assimilated meteorological fields. *J. Geophys. Res.-Atmos.* 106, 12109–12128.
- Liu, C., Watanabe, M., Wang, Q., 2008. Changes in nitrogen budgets and nitrogen use efficiency in the agroecosystems of the Changjiang River basin between 1980 and 2000. *Nutr. Cycl. Agroecosyst.* 80, 19–37.
- Liu, X.J., Duan, L., Mo, J.M., Du, E.Z., Shen, J.L., Lu, X.K., Zhang, Y., Zhou, X.B., He, C.E., Zhang, F.S., 2011. Nitrogen deposition and its ecological impact in China: an overview. *Environ. Pollut.* 159 (10), 2251–2264.
- Liu, X.J., Zhang, Y., Han, W.X., Tang, A.H., Shen, J.L., Cui, Z.L., Vitousek, P., Erisman, J.M., Goulding, K., Christie, P., 2013. Enhanced nitrogen deposition over China. *Nature* 494 (7438), 459–462.
- Liu, X.J., Xu, W., Pan, Y.P., Du, E.Z., 2015. Liu et al. suspect that Zhu, et al. (2015) may have underestimated dissolved organic nitrogen (N) but overestimated total particulate N in wet deposition in China. *Sci. Total Environ.* 520, 300–301.
- Liu, L., Zhang, X.Y., Wang, S.Q., Lu, X.H., Ouyang, X.Y., 2016a. A review of spatial variation of inorganic nitrogen (N) wet deposition in China. *Plos One* 11 (1), e0146051.
- Liu, X.J., Vitousek, P., Chang, Y.H., Zhang, W.F., Matson, P., Zhang, F.S., 2016b. Evidence for a historic change occurring in China. *Environ. Sci. Technol.* 50 (2), 505–506.
- Liu, X.J., Xu, W., Duan, L., Du, E.Z., Pan, Y.P., Lu, X.K., Zhang, L., Wu, Z.Y., Wang, X.M., Zhang, Y., Shen, J.L., Song, L., Feng, Z.Z., Liu, X.J., Song, W., Tang, A.H., Zhang, Y.Y., Zhang, X.Y., Collett, J.L., 2017. Atmospheric nitrogen emission, deposition, and air quality impacts in China: an Overview. *Curr. Pollut. Rep.* <https://doi.org/10.1007/s40726-017-0053-9>.
- Mari, C., Jacob, D.J., Bechtold, P., 2000. Transport and scavenging of soluble gases in a deep convective cloud. *J. Geophys. Res.-Atmos.* 105, 22255–22267.
- Martin, R.V., Jacob, D.J., Yantosca, R.M., Chin, M., Ginoux, P., 2003. Global and regional decreases in tropospheric oxidants from photochemical effects of aerosols. *J. Geophys. Res.* 108, 4097. <https://doi.org/10.1029/2002JD002622>.
- Neff, J.C., Holland, E.A., Dentener, F.J., McDowell, W.H., Russell, K.M., 2002. The origin, composition and rates of organic nitrogen deposition: a missing piece of nitrogen cycle? *Biogeochemistry* 57/58 (1), 99–136.
- Nowlan, C.R., Martin, R.V., Philip, S., Lamsal, L.N., Krotkov, N.A., Marais, E.A., Wang, S., Zhang, Q., 2014. Global dry deposition of nitrogen dioxide and sulfur dioxide inferred from space-based measurements. *Glob. Biogeochem. Cy.* 28 (10), 1025–1043.
- Oxley, T., Dore, A.J., Kryza, M., ApSimon, H., 2013. Modelling future impacts of air pollution using the multi-scale UK Integrated Assessment Model (UKIAM). *Environ. Int.* 61, 17–37.
- Pan, Y.P., Wang, Y.S., Tang, G.Q., Wu, D., 2012. Wet and dry deposition of atmospheric nitrogen at ten sites in Northern China. *Atmos. Chem. Phys.* 12 (14), 6515–6535.
- Qiao, X., Tang, Y., Kota, S.H., Li, J.Y., Wu, L., Hu, J.L., Zhang, H.L., Ying, Q., 2015. Modeling dry and wet deposition of sulfate, nitrate, and ammonium ions in Jiuzhaigou National Nature Reserve, China using a source-oriented CMAQ model: Part II. Emission sector and source region contributions. *Sci. Total Environ.* 532, 840–848.
- Shen, J.L., Li, Y., Liu, X.J., Luo, X.S., Tang, H., Zhang, Y.Z., Wu, J.S., 2013. Atmospheric dry and wet nitrogen deposition on three contrasting land use types of an agricultural catchment in subtropical central China. *Atmos. Environ.* 67 (2), 415–424.
- Simpson, D., Andersson, C., Christensen, J.H., Engardt, M., Geels, C., Nyiri, A., Posch, M., Soares, J., Sofiev, M., Wind, P., 2014. Impacts of climate and emission changes on nitrogen deposition in Europe: a multi-model study. *Atmos. Chem. Phys.* 13, 6995–7017.
- Song, L., Kuang, F.H., Skiba, U., Zhu, B., Liu, X.J., Levy, P., Dore, A.J., Fowler, D., 2017. Bulk deposition of organic and inorganic nitrogen in southwest China from 2008 to 2013. *Environ. Pollut.* 227, 157–166.
- Vet, R., Artz, R.S., Carou, S., Shaw, M., Ro, C.-U., Aas, W., Baker, A., Bowersox, V.C., Dentener, F., Galy-Lacaux, C., Hou, A., Pienaar, J.J., Gillett, R., Cristina Forti, M., Gromov, S., Hara, H., Khodzher, T., Mahowald, N.M., Nickovic, S., Rao, P.S.P., Reid, N.W., 2014. A global assessment of precipitation, chemistry and deposition of sulfur, nitrogen, sea salt, base cations, organic acids, acidity and pH, and phosphorus. *Atmos. Environ.* 93 (3–4), 3–100.
- Veuger, B., Middelburg, J.J., Boschker, H.T.S., Nieuwenhuize, J., Rijswijk, P.V., Rochelle-Newall, E.J., Navarro, N., 2004. Microbial uptake of dissolved organic and inorganic nitrogen in Randers Fjord. *Estuar. Coast. Shelf Sci.* 61 (3), 507–515.
- Wang, Q.X., Koshikawa, H., Liu, C., Otsubo, K., 2014. 30-year changes in the nitrogen inputs to the Yangtze River Basin. *Environ. Res. Lett.* 9 (11), 115005.
- Wesely, M.L., 1989. Parameterization of surface resistances to gaseous dry deposition in regional-scale numerical models. *Atmos. Environ.* 23, 1293–1304.
- Xiao, H.Y., Tang, C.G., Xiao, H.W., Liu, X.Y., Liu, C.Q., 2010. Mosses indicating atmospheric nitrogen deposition and sources in the Yangtze River drainage basin, China. *J. Geophys. Res.* 115 (D14), 1307–1314.
- Xu, J., Yang, D., Yi, Y., Lei, Z., Chen, J., Yang, W., 2008. Spatial and temporal variation of runoff in the Yangtze River basin during the past 40 years. *Quat. Int.* 186 (1), 32–42.
- Xu, H., Chen, Z.Y., Finlayson, B., Webber, M., Wu, X.D., Li, M.T., Chen, J., Wei, T.Y., Barnett, J., Wang, M., 2013. Assessing dissolved inorganic nitrogen flux in the Yangtze River, China: sources and scenarios. *Glob. Planet. Chang.* 106 (4), 84–89.
- Xu, W., Luo, X.S., Pan, Y.P., Zhang, L., Tang, A.H., Shen, J.L., Zhang, Y., Li, K.H., Wu, Q.H., Yang, D.W., Zhang, Y.Y., Xue, J., Li, W.Q., Li, Q.Q., Tang, L., Lu, S.H., Liang, T., Tong, Y.A., Liu, P., Zhang, Q., Xiong, Z.Q., Shi, X.J., Wu, L.H., Shi, W.Q., Tian, K., Zhong, X.H., Shi, K., Tang, Q.Y., Zhang, L.J., Huang, J.L., He, C.E., Kuang, F.H., Zhu, B., Liu, H., Jin, X., Xin, Y.J., Shi, X.K., Du, E.Z., Dore, A.J., Tang, S., Collett, J.L., Goulding, K., Sun, Y.X., Ren, J., Zhang, F.S., Liu, X.J., 2015. Quantifying atmospheric nitrogen deposition through a nationwide monitoring network across China. *Atmos. Chem. Phys.* 15 (13), 12345–12360.
- Yan, W.J., Zhang, S., Sun, P., Seitzinger, S.P., 2003. How do nitrogen inputs to the Changjiang basin impact the Changjiang River nitrate: a temporal analysis for 1968–1997. *Glob. Biogeochem. Cy.* 17 (4), 2–1.
- Zhang, L., Gong, S., Padro, J., Barrie, L., 2001. A size-segregated particle dry deposition scheme for an atmospheric aerosol module. *Atmos. Environ.* 35 (3), 549–560.
- Zhang, L., Jacob, D.J., Knipping, E.M., Kumar, N., Munger, J.W., Carouge, C.C., van Donkelaar, A., Wang, Y.X., Chen, D., 2012a. Nitrogen deposition to the United States: distribution, sources, and processes. *Atmos. Chem. Phys.* 12 (10), 4539–4554.
- Zhang, Y., Song, L., Liu, X.J., Li, W.Q., Lü, S.H., Zheng, L.X., Bai, Z.C., Cui, G.Y., Zhang, F.S., 2012b. Atmospheric organic nitrogen deposition in China. *Atmos. Environ.* 46 (3), 195–204.
- Zhao, B., Wang, S.X., Liu, H., Xu, J.Y., Fu, K., Klimont, Z., Hao, J.M., He, K.B., Cofala, J., Amann, M., 2013. NO_x emissions in China: historical trends and future perspectives. *Atmos. Chem. Phys.* 13 (6), 16047–16112.
- Zhao, Y., Zhang, L., Pan, Y., Wang, Y., Paulot, F., Henze, D.K., 2015. Atmospheric nitrogen deposition to the northwestern Pacific: seasonal variation and source attribution. *Atmos. Chem. Phys.* 15 (9), 10905–10924.
- Zhao, Y., Zhang, L., Chen, Y.F., Liu, X.J., Xu, W., Pan, Y.P., Duan, L., 2017. Atmospheric nitrogen deposition to China: a model analysis on nitrogen budget and critical load exceedance. *Atmos. Environ.* 153, 32–40.